

AD-A100 724

TECHNICAL  
LIBRARY

AD

MEMORANDUM REPORT ARBRL-MR-03095

MEASUREMENTS OF DYNAMIC STRESS AND  
STRAIN COMPONENTS IN TARGETS  
STRUCK BY PENETRATORS

Dennis S. Pritchard

March 1981



US ARMY ARMAMENT RESEARCH AND DEVELOPMENT COMMAND  
BALLISTIC RESEARCH LABORATORY  
ABERDEEN PROVING GROUND, MARYLAND

Approved for public release; distribution unlimited.

DTIC QUALITY INSPECTED 3

Destroy this report when it is no longer needed.  
Do not return it to the originator.

Secondary distribution of this report by originating  
or sponsoring activity is prohibited.

Additional copies of this report may be obtained  
from the National Technical Information Service,  
U.S. Department of Commerce, Springfield, Virginia  
22161.

The findings in this report are not to be construed as  
an official Department of the Army position, unless  
so designated by other authorized documents.

*The use of trade names or manufacturers' names in this report  
does not constitute endorsement of any commercial product.*

**UNCLASSIFIED**

SECURITY CLASSIFICATION OF THIS PAGE (When Data Entered)

<b>REPORT DOCUMENTATION PAGE</b>		<b>READ INSTRUCTIONS BEFORE COMPLETING FORM</b>
1. REPORT NUMBER MEMORANDUM REPORT ARBRL-MR-03095	2. GOVT ACCESSION NO.	3. RECIPIENT'S CATALOG NUMBER
4. TITLE (and Subtitle) Measurements of Dynamic Stress and Strain Components in Targets Struck by Penetrators		5. TYPE OF REPORT & PERIOD COVERED Jun 77 - Jun 79
7. AUTHOR(s) Dennis S. Pritchard		6. PERFORMING ORG. REPORT NUMBER
9. PERFORMING ORGANIZATION NAME AND ADDRESS USA Ballistic Research Laboratory Aberdeen Proving Ground, MD 21005		10. PROGRAM ELEMENT, PROJECT, TASK AREA & WORK UNIT NUMBERS DA Proj. No. 1L161102AH43
11. CONTROLLING OFFICE NAME AND ADDRESS USA ARRADCOM, Ballistic Research Laboratory ATTN: DRDAR-BL Aberdeen Proving Ground, MD 21005		12. REPORT DATE MARCH 1981
14. MONITORING AGENCY NAME & ADDRESS(if different from Controlling Office)		13. NUMBER OF PAGES 33
		15. SECURITY CLASS. (of this report) Unclassified
		15a. DECLASSIFICATION/DOWNGRADING SCHEDULE
16. DISTRIBUTION STATEMENT (of this Report) Approved for Public Release; distribution unlimited.		
17. DISTRIBUTION STATEMENT (of the abstract entered in Block 20, if different from Report)		
18. SUPPLEMENTARY NOTES		
19. KEY WORDS (Continue on reverse side if necessary and identify by block number) Dynamic Stress, Dynamic Strain, Penetration, Ballistic Impact, Kinetic Energy Projectiles, Manganin Gauge, Strain Gauge, Rolled Homogeneous Armor, RHA		
20. ABSTRACT (Continue on reverse side if necessary and identify by block number) bet/2972 Stress and strain profiles have been recorded in targets impacted by long-rod kinetic-energy projectiles. Stress gauge records were strongly influenced by the strain field in the target, so compensating strain measurements were used to derive the correct stress profile. Strain-compensated stress gauges in the projectile path measured stress which increased to a value that remained nearly constant until penetration neared the gauge. This constant stress was close to the value of the Hugoniot Elastic Limit of the target material.		

## TABLE OF CONTENTS

	<u>Page</u>
TABLE OF CONTENTS . . . . .	3
LIST OF ILLUSTRATIONS . . . . .	5
I. INTRODUCTION . . . . .	7
II. BACKGROUND . . . . .	7
III. EXPERIMENTS AND RESULTS . . . . .	9
A. Stress-Gauge Circuit . . . . .	11
B. Test 1 . . . . .	11
C. Tests 2 & 3 . . . . .	13
D. Tests 9 & 13 . . . . .	13
E. Tests 15 & 16 . . . . .	20
IV. SUMMARY AND CONCLUSION . . . . .	24
ACKNOWLEDGEMENTS . . . . .	25
REFERENCES . . . . .	26
DISTRIBUTION LIST . . . . .	27

## LIST OF ILLUSTRATIONS

<u>FIG. NO.</u>		<u>Page</u>
1	Stress Waves in a 'Perspex' Plate. . . . .	8
2	Circuit Schematic. . . . .	12
3	Tests 2 & 3 - Experimental Setup . . . . .	14
4	Stress-Time Histories for Tests 2 & 3. . . . .	15
5	Test 9 - Experimental Setup. . . . .	16
6	Test 13 - Experimental Setup . . . . .	18
7	Stress and Strain Histories for Tests 9 & 13 . . . . .	19
8	Tests 15 & 16 - Experimental Setup . . . . .	21
9	Stress and Strain Histories for Tests 15 & 16. . . . .	23

## I. INTRODUCTION

Experiments have been performed to measure the stress developed in targets during penetration by long-rod projectiles. This investigation is part of a continuing effort to characterize the complete behavior of targets and projectiles during the penetration process. Hard steel rods were used as the projectile; several materials were used as targets. Saboted projectiles were launched from a 100-mm light-gas gun at velocities from 750 to 1000 m/s and impacted the face of right-cylindrical targets at normal incidence. Stress developed during penetration was measured by gauges located along the penetration path in the targets. Measurements began with the arrival of the initial shock and should have continued until penetration reached the gauge location. Although this measurement objective was not fully achieved, there was significant progress. This report provides background information, describes the evolution of experimental procedures, presents results, and discusses various problem areas.

## II. BACKGROUND

Some insight into the behavior of targets during penetration has been gained by examining prior work. The reaction of a target to point-initiated impulsive loading is indicated in Figure 1<sup>1</sup>. This figure shows a series of time-lapse photographs of an explosive pellet detonated against a 'Perspex'\* plate. The detonation initiates a strong shock pulse in the material. This shock progresses through the material, with stress relief from the lateral boundaries. The spherical wave front approaches the back surface, reflects from it, and returns as a rarefaction into the stressed material. The last two frames in the figure indicate the complicated wave interactions which result as time progresses. This phenomenon occurs when a single pulse of energy, deposited in one area, propagates throughout the target. When a kinetic-energy penetrator strikes a target, energy is delivered to the target in a continuous manner over a long time. More complicated target interactions occur as both target and penetrator materials deform and fail, and stress and strain fields that develop behind the initial shock front have not been well defined. In this investigation, the stress history behind the expanding shock front has been monitored in the path of penetration. The measurements have been performed using gauges located at different depths within several types of targets.

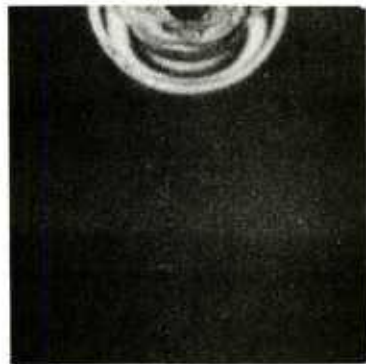
---

<sup>1</sup>H. Kolsky, *Stress Waves in Solids*, Dover Publications, Inc., New York, 1963, Plate I.

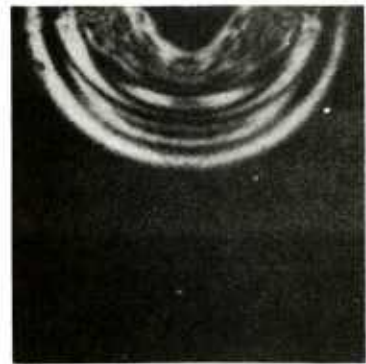
\*Trade Name for PMMA.



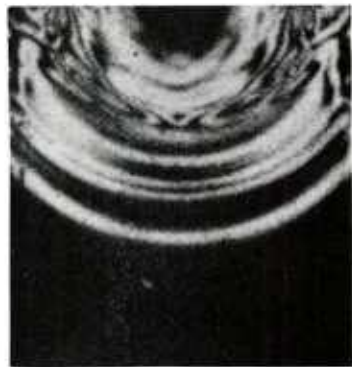
1. 0  $\mu$ sec.



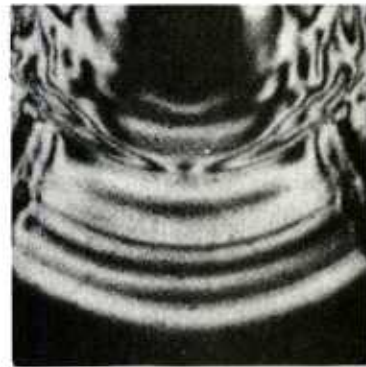
2. 10.5  $\mu$ sec.



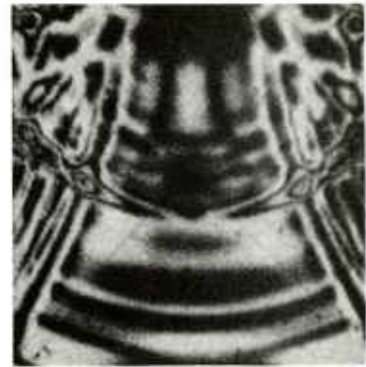
3. 21.7  $\mu$ sec.



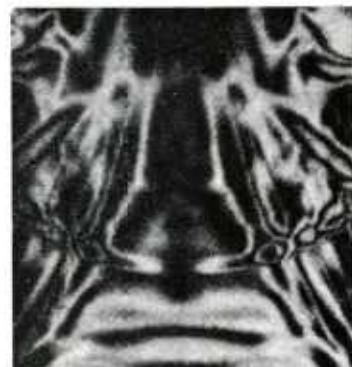
4. 34.3  $\mu$ sec.



5. 47.3  $\mu$ sec.



6. 60.8  $\mu$ sec.



7. 72.7  $\mu$ sec.



8. 84.7  $\mu$ sec.



9. 93.5  $\mu$ sec.

Figure 1. Stress Waves in a 'Perspex' Plate.

The problem of making stress measurements in targets has been investigated by Charest<sup>2</sup>. In his experiments, stress was generated in layered targets by the hypervelocity impact of metal spheres. Typical stress-time data at various stations in the targets indicated an initial pulse-type loading of the gauges, after which the stress decreased to a steady-state condition, which continued until the gauge was destroyed. In a more recent study by Charest<sup>3</sup>, a layered target of PMMA was impacted at low-velocity by a 22-caliber bullet. Stress produced in the target was monitored by a single gauge. Results showed that stress in the PMMA target increased rapidly in a linear manner until the gauge was destroyed.

### III. EXPERIMENTS AND RESULTS

The experimental series reported here was evolutionary. Techniques were continually modified to improve the experimental results from each test. Major problems were solved. For example, stress gauges were used exclusively until it was decided that a strain gauge must also be included to monitor strain. An initial test was conducted which involved explosively loading an instrumented target. In all subsequent experiments, penetration into various instrumented targets by long rods was conducted. Penetrators were composed of S-7 tool steel (RC 40), except in Test 2 where drill rod was used. All penetrators were 254 mm long and 8.1 mm in diameter. Circular targets (19.0-88.9 mm thick and 101.6 mm diameter) of yellow brass, mild steel, and rolled homogeneous armor (RHA) were impacted. Target configurations varied. Gauge locations in the targets were measured from the target impact surface. Manganin foil gauges measured stress and Constantan foil gauges measured strain. The Manganin gauges for the first seven tests were double bifilar gauges<sup>4</sup>. All subsequent stress and strain gauges used were simpler<sup>5</sup>. Mica, aluminum oxide, and Kapton sheets (0.013-2.758 mm thick) were tested as insulators between gauges and targets. Mica and aluminum oxide were too brittle for the large deformation in these experiments. The best insulator was Kapton (0.127 mm thick). A summary of experimental data is shown in Table 1. The circuit description for these experiments follows.

---

<sup>2</sup>J. A. Charest, "Measurements of Hypervelocity Impact Pressures Using In-Material Manganin Gauges," EG&G Report S-487-k, Santa Barbara Division, April 1970.

<sup>3</sup>J. A. Charest, "Development of a Strain-Compensated Shock Pressure Gauge," Dynasen, Inc. TR 005, February 1979.

<sup>4</sup>A. V. Anan'in, A. N. Dremin, and G. I. Kanel', "Structure of Shock and Rarefaction Waves in Iron," Fizika Gorenija i Vzryva, Vol. 9, No. 3, May-June 1973, pp. 437-43.

<sup>5</sup>E. O. Williams, "An Etched Manganin Gauge System for Shock-Pressure Measurement in a High-Noise Environment," ISA Transaction, Vol. 7, No. 3, 1968, pp. 223-30.

Test Number	Initial Projectile Velocity (m/s)	Target Material	Target Thickness (mm)	Gauge Location(s) (mm)	Measured Signal Duration (μs)	Peak Stress (GPa)	Strain Gage (peak percent)
1	---	RJIA	9.45	6.22	5	---	No
2	840	"	25.40	12.70	18	6.8	"
3	1,000	"	"	"	19	12.0	"
4	"	"	54.00	28.60	13	0.4	"
5	"	"	38.10	25.40	6	3.5	"
6	"	"	"	"	8	0.6	"
7	"	"	24.56	18.21	0.5	10.0	"
8	750	Yellow Brass	96.24	53.70	31	13.1	"
9	"	"	95.78	52.04	30	4.6	Yes (21.4)
10	---	"	93.22	51.08	---	---	Yes (---)
11	750	"	94.84	52.83	5	60.0	No
12	"	"	86.46	42.06	147	25.0	"
13	"	"	88.90	44.45	184	7.2	"
14	"	"	"	"	---	---	Yes (---)
15	1,000	1018 Steel	50.80	25.40	100	19.8	Yes (26.0)
16	1,000	1020 Steel	"	"	18	2.8	Yes (2.3)

TABLE I - Summary Table of Experimental Data.

### A. Stress-Gauge Circuit.

Stress was measured by the bridge circuit shown in Figure 2. A 50-ohm stress gauge was connected to one leg of the bridge by approximately 10 meters of RG 213/U coaxial cable. The bridge was dynamically balanced by adjusting the 5-turn, 100-ohm potentiometer, and was powered by a 300-volt direct current source which was triggered at least 10  $\mu$ s before projectile impact. Calibrations for expected stress levels were obtained by triggering the circuit with various resistors in series with the stress gauge. During calibrations, a crowbar across the gauge leg of the bridge interrupted the current flow after approximately 50  $\mu$ s to protect the gauge from excessive heating. (Most calibrations were also performed with a dummy gauge which was substituted to avoid possible damage to the test gauge.) Changes in resistance during a test were converted to stress using a stress-gauge calibration based on measurements by Charest<sup>6</sup>. A similar circuit was used in later experiments to measure the associated strain. Calibrations for expected strain levels were obtained by triggering the strain gauge circuit with various resistors in parallel with the strain gauge. Placing calibrating resistors in parallel with the strain gauge rather than in series yields more accurate calibrations. Data reduction utilized the circuit equation so that calibrations could be based on decreasing gauge resistance, while the actual measurements encountered increasing gauge resistance.

### B. Test 1.

A shock experiment was conducted while awaiting parts for penetration experiments. This experiment was intended to test construction concepts and to yield a stress history similar to that encountered in the target of Figure 1. A PBX pellet was detonated, initiating a shock pulse in a thin RHA plate. A double bifilar stress gauge, sandwiched between this plate and another thin RHA piece, monitored stress. This type of gauge, patterned after noninductive gauges designed by other investigators<sup>4</sup>, was introduced in an effort to prevent electrical noise induced by magnetic changes in the ferromagnetic target. Hauver encountered this form of noise in some of his work with rolled homogeneous armor at the Ballistic Research Laboratory (BRL)<sup>7</sup>. Unfortunately, the power supply failed to trigger and no stress history was recorded. A weak signal was generated due to slight gauge effects induced by target shock. This signal was sufficiently clean and the time duration was long enough, indicating this experimental construction was a type that showed promise.

---

<sup>6</sup>J. A. Charest, "Characterization of an Encapsulated 50-Ohm Manganin Foil Piezoresistive Gauge", Air Force Weapons Laboratory Technical Report No. AFWL-71-81, Kirtland Air Force Base, August 1972.

<sup>7</sup>G. E. Hauver, "The Alpha-Phase Hugoniot of Roll Homogeneous Armor", BRL Memorandum Report No. 2651, Ballistic Research Laboratory, Aberdeen Proving Ground, MD, August 1976, p. 14.

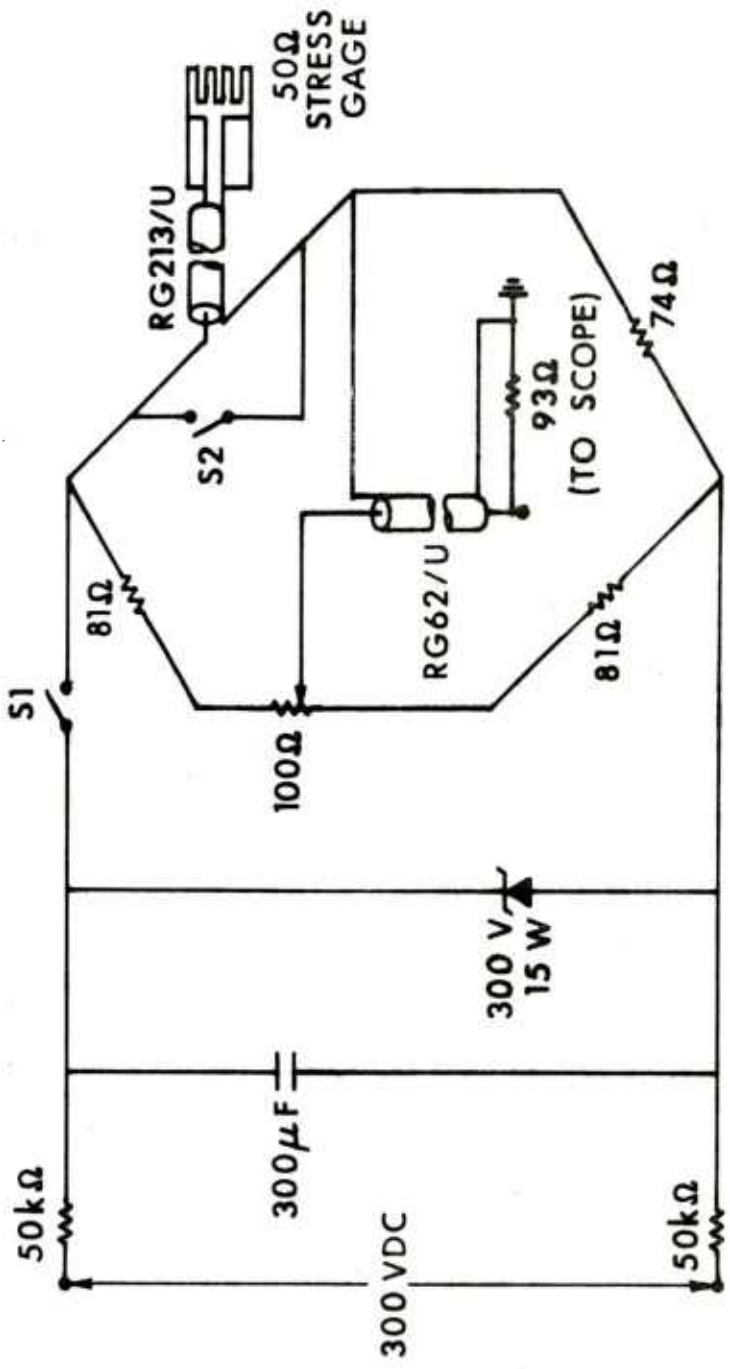


Figure 2. Circuit Schematic.

This shock experiment was not repeated since long-rod penetration was the primary consideration in this investigation.

C. Tests 2 & 3.

Stress measurements were next attempted in layered RHA targets as they were penetrated by long steel rods. An exploded view of the experimental setup for Tests 2 and 3 is shown in Figure 3. The stress gauge was sandwiched between RHA plates with its active element centered on the axis of penetration. Mica sheets, 0.015 mm thick, insulated the gauge from the surrounding RHA. The target assembly was bonded together with epoxy cement; bond thicknesses were less than 0.003 mm. Tests 2 and 3 were identical, except for the projectile striking velocity, which was 840 m/s in Test 2 and 1000 m/s in Test 3.

Stress-time histories measured in Tests 2 and 3 are shown in Figure 4. The signal from Test 2 was initially troubled by electrical noise, but suggested a nearly linear increase in stress to nearly 3.0 GPa before the gauge was destroyed at approximately 18  $\mu$ s. The curve for Test 3 suggests a more rapid increase in stress to a maximum value near 12.0 GPa before the gauge was destroyed at approximately 16  $\mu$ s. For penetration to reach the gauge location in these times, penetration would have to proceed at over three-fourths of the impact velocity, which is unreasonably high. The results from Tests 2 and 3, therefore, suggest that gauge leads probably fail before penetration reaches the gauge location. Lead failure was probably caused by shear in the layered targets.

D. Tests 9 & 13.

Experiments were performed in an effort to devise a target configuration that eliminates the shear problem in these tests. For the four tests following Test 3, each RHA target configuration was changed in an unsuccessful attempt to eliminate the shear problem. In the next seven tests, brass target material was used to save experimental construction time during this crucial development phase of testing. The brass targets were easier to machine, which saved time. Brass is not a magnetically susceptible material, so it was not envisioned that the simple gauges used would encounter significant noise. The use of simple gauges in these targets simplified target assembly procedures, again saving valuable time. A new addition in some of these experiments was the placement of a strain gauge in the area of the stress gauge to record a concurrent strain-time history. More experimental information was gained for each test with this addition. This addition is indicated in Figure 5, which shows the experimental setup for Test 9. Several tests with the same basic target configuration indicated in Figure 5 were conducted with varied amounts of success. Test 9 produced the best results for this basic configuration. It was not foreseen before Test 9 was conducted that the addition of a strain gauge to a test was extremely important. A target arrangement that was tried for the first time in Test 13 is

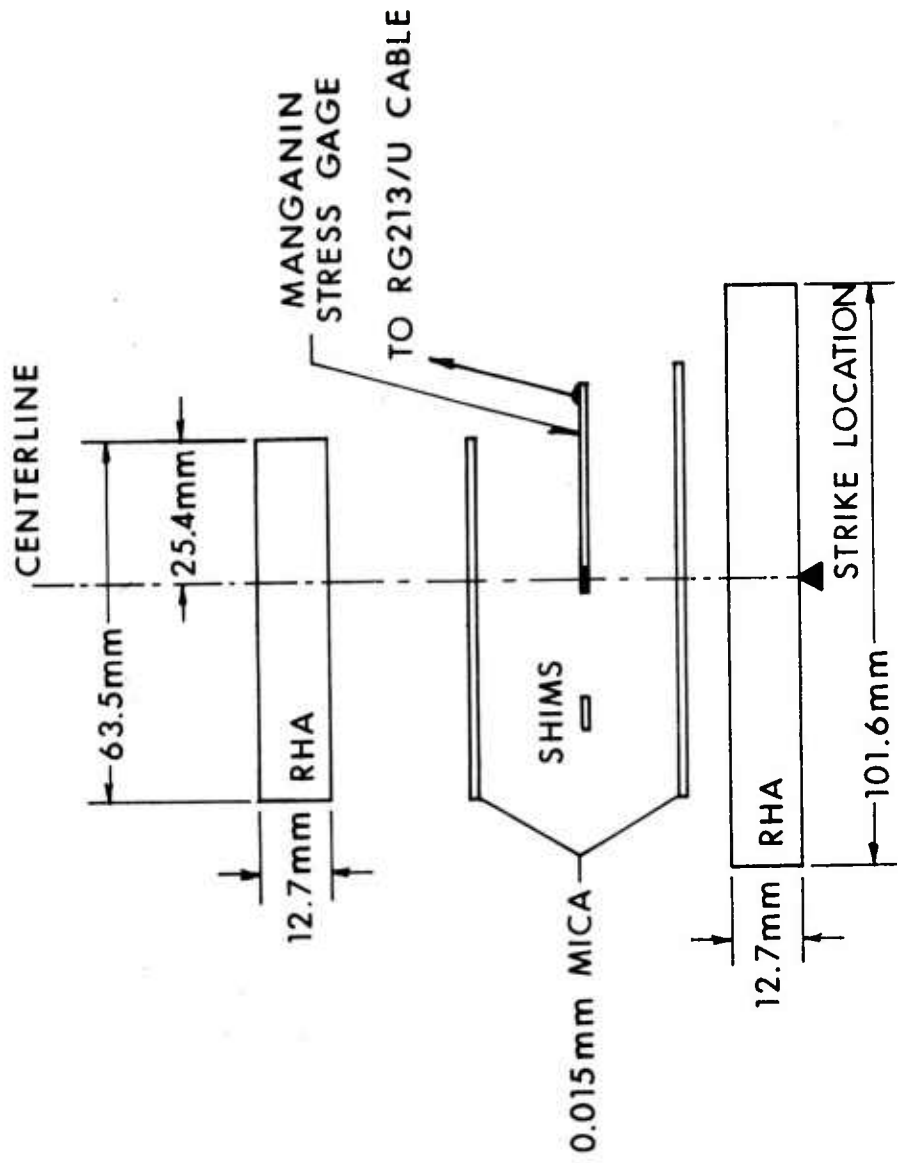


Figure 3. Tests 2 & 3 - Experimental Setup.

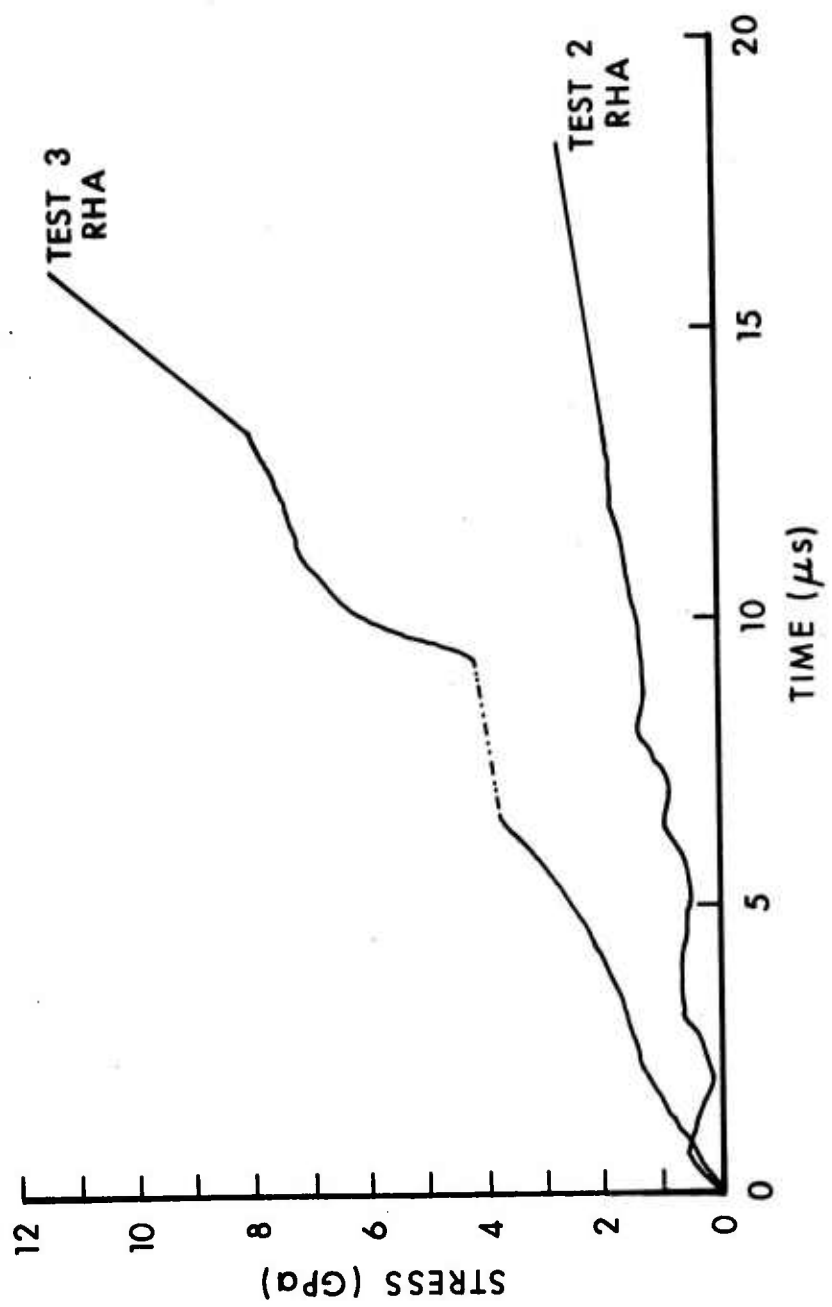


Figure 4. Stress-Time Histories for Tests 2 & 3.

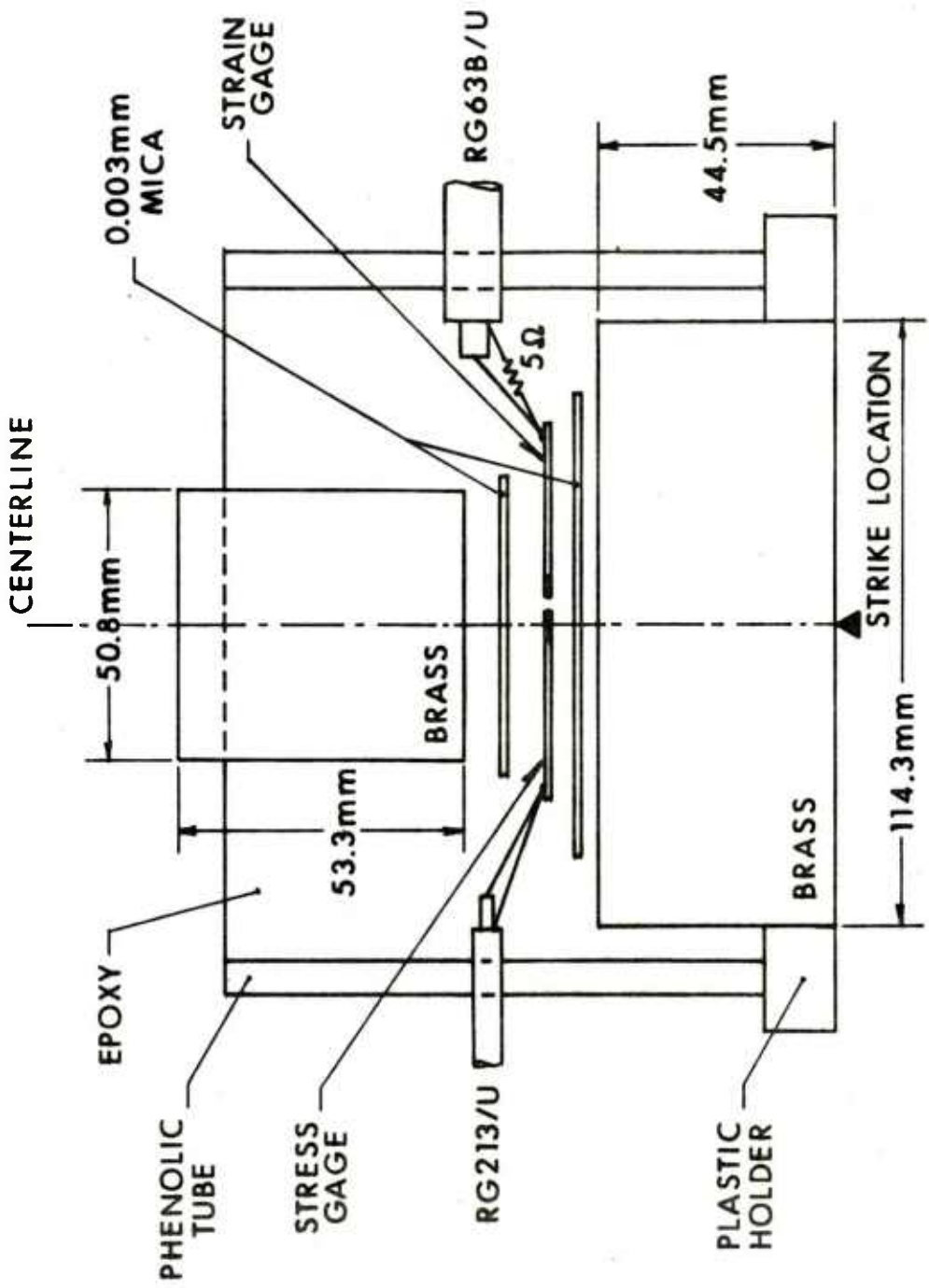


Figure 5. Test 9 - Experimental Setup.

illustrated in Figure 6. A round monobloc target was used, with a single hole drilled through it as represented in the cross-sectional view. A stress gauge was sandwiched between two brass half-round rods. Kapton sheets provided insulation between the gauges and the rods. This complete rod assembly was then slipped into the drilled hole to align the active element area of the gauge along the penetration path of the projectile. This insertion technique is similar to a method that was employed at the Ballistic Research Laboratory by Netherwood<sup>8</sup>. A vacuum technique was used to extrude epoxy uniformly around the rods and the gauge. Then the complete target setup was placed in an oven at 353°K for two hours to cure the epoxy, which held all target components in their correct positions. Proper application and curing of the epoxy also eliminates voids between these components. Void elimination is a critical factor in these experiments because voids located in critical areas can cause premature gauge failures. Also, the small drilled hole (6.4 mm diameter) gave the target more integrity than in previous tests.

Results from Tests 9 and 13 are shown in Figure 7, forming the basis for a comparison of the relative validity of these two experiments. The stress-time histories for Tests 9 and 13 are graphed as in Figure 4 and the strain-time history for the strain gauge in Test 9 is also represented. The total mass penetrated along the centerline for Test 9 was nearly the same as for Test 13. The gauges for Tests 9 and 13 were located at the same depths within their respective targets. Initial projectile velocities for all tests using brass targets was 750 m/s. A vast difference exists between stress-time histories that should be identical, based on these similar conditions for both experiments. The stress-time curve from Test 9 has a steep slope and a short time duration. The stress-time curve from Test 13 has a much longer duration than that from Test 9 and a slightly curved slope. The rapidly changing form on the end of the Test 13 stress record is probably an artifact of the destruction of the gauge by the projectile. Test 9 is suspect. When the stress-time and strain-time records for this test are compared, a large time difference between the ends of the records is found. This difference suggests that the leads for the stress and strain gauges failed at different times. The stress gauge leads for Test 9 also failed much earlier than in Test 13, which is an even stronger indication that the use of the Test 9 experimental setup did not solve the shearing problem. Also, slippage between target plates during penetration may have adversely affected measurements in Test 9. The gauge leads in Test 13 were extended and partially isolated from the target. This isolation left the critical cable connection areas free from severe deformation caused by penetration, eliminating the shear problem in these experiments. Test 13 produced the most accurate measurements that were made up to that point in the test series, due in part to the extended gauge lead life during that test.

---

<sup>8</sup>P. H. Netherwood, "Rate of Penetration Measurements", BRL Memorandum Report ARBRL-MR-02978, Ballistic Research Laboratory, Aberdeen Proving Ground, MD, December 1979, p. 15.

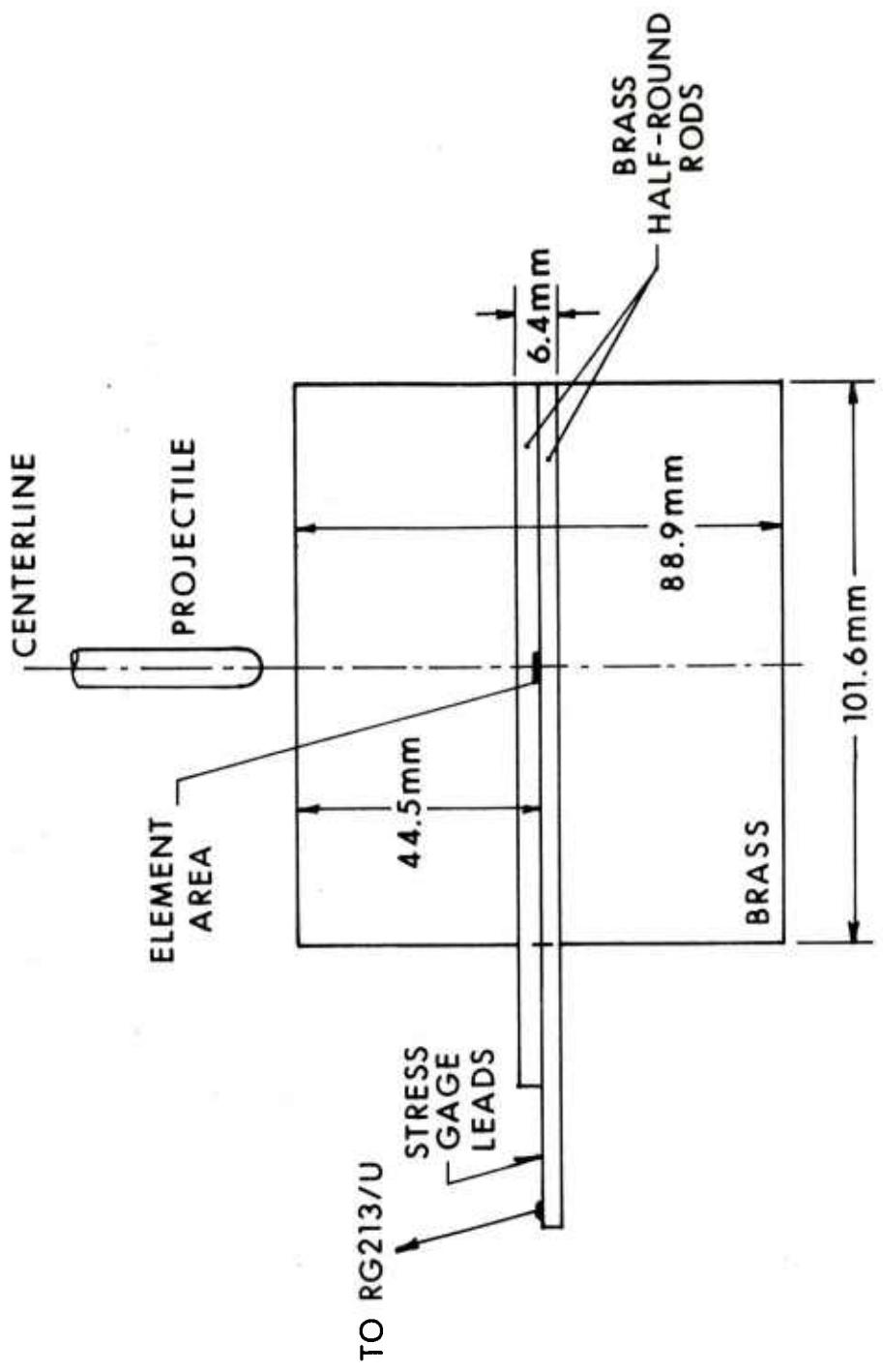


Figure 6. Test 13 - Experimental Setup.

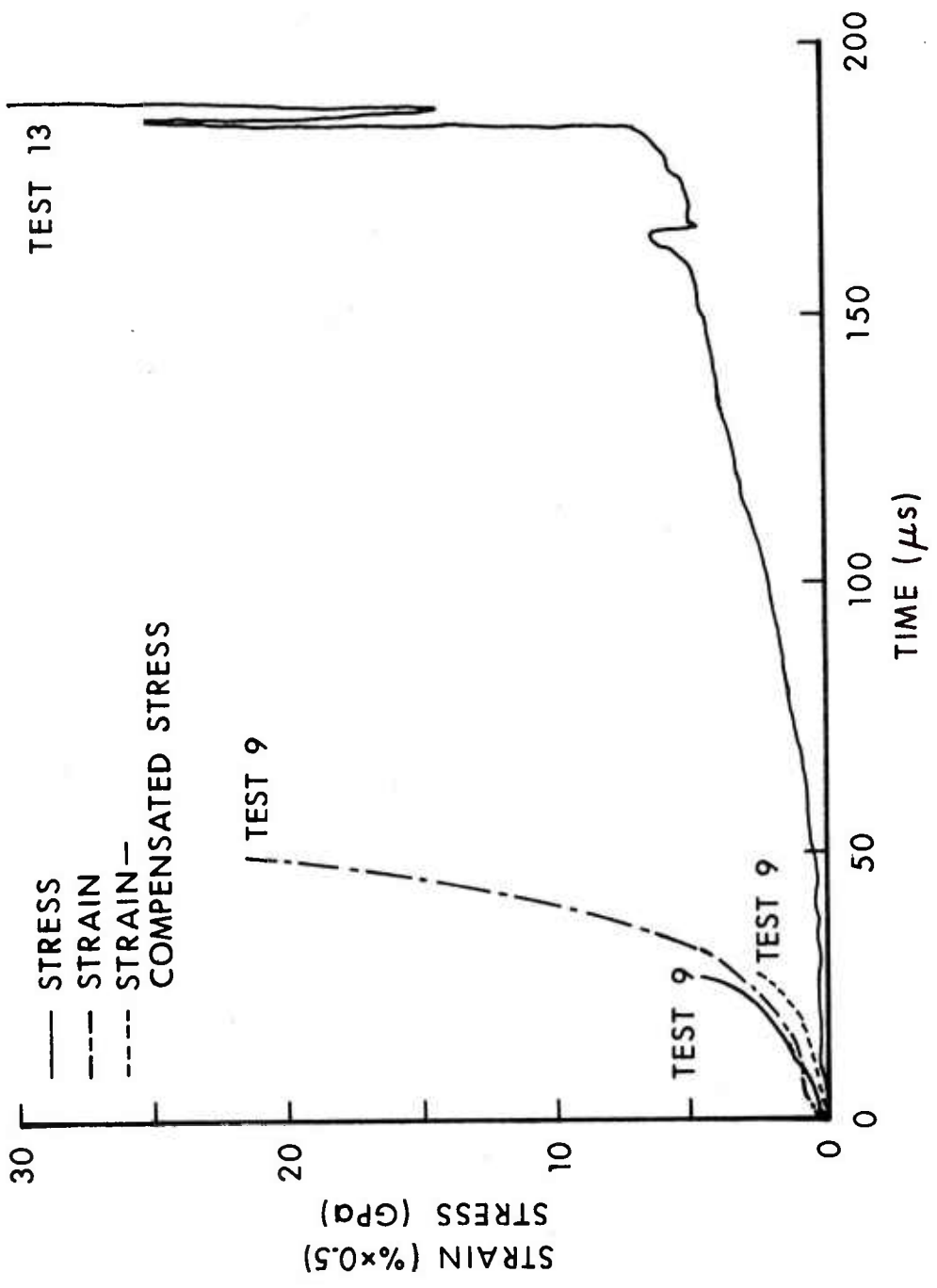


Figure 7. Stress and Strain Histories for Tests 9 & 13.

The spherically divergent strain encountered in the penetration experiments in this report had an effect on the stress gauges used. Both Charest and Trimble discovered a "false" component in a stress signal when the stress gauge producing that signal was simultaneously stressed parallel to the projectile motion and strained perpendicular to the projectile motion (spherically divergent strain) during penetration<sup>3,9</sup>. This divergent strain, inducing a strain gauge effect in the stress gauge, contributes to a significant amount of the change in resistance of the stress gauges in these experiments. This contribution forms the false components in the stress gauge signals that were analyzed. The strain gauge effect in the stress gauge required the introduction of a proper method of data reduction to adjust for this effect. For Test 9, values of strain from the resulting strain-time curve were analyzed with respect to the values of stress that occur at the corresponding times on the stress-time curve. Each value of strain was introduced into a standard equation ( $\Delta R/R_0 = G\epsilon$ ), with the proper strain coefficient for the stress gauge (G), to yield the correct change in resistance that defines the false signal value measured by the stress gauge at that time. Then the false signal value was subtracted from the measured stress signal value, resulting in a single value that was analyzed to yield the true stress (strain-compensated) in the direction of projectile penetration. Complete analysis along the strain-time and stress-time curves for Test 9 produced the strain-compensated stress curve shown in Figure 7.

#### E. Tests 15 and 16.

The experimental configuration for Test 13 was extended for all subsequent tests because this configuration yields the best experimental results. The experimental setup for the most recent tests (15 & 16) is represented in Figure 8. The initial projectile velocity for both tests was 1,000 m/s. There were only two major changes in the target configuration for both tests with respect to Test 13. In one of these changes, a strain gauge was placed opposite the stress gauge as for Test 9, but the active element area of the strain gauge was in register with the active element area of the stress gauge. This arrangement allowed the gauges to record exactly the same phenomenon. The other change was the use of mild steel targets. Simple gauges were still used, though they are susceptible to magnetically induced noise. Use of these gauges required two simple, yet effective, techniques to shield the active element areas from this induced noise. First, the continued use of the half-round brass rods allowed the gauges a large standoff distance from the steel. Also, brass has a very low magnetic susceptibility. The standoff distance involved and the magnetic properties of the brass drastically reduced the amount of noise-producing magnetic flux allowed

---

<sup>9</sup>J. J. Trimble, "Manganin Gage Pressure Measurements Under Conditions Where Gage Deformation Occurs", BRL Technical Report ARBRL-TR-02180, Ballistic Research Laboratory, Aberdeen Proving Ground, MD, July 1979.

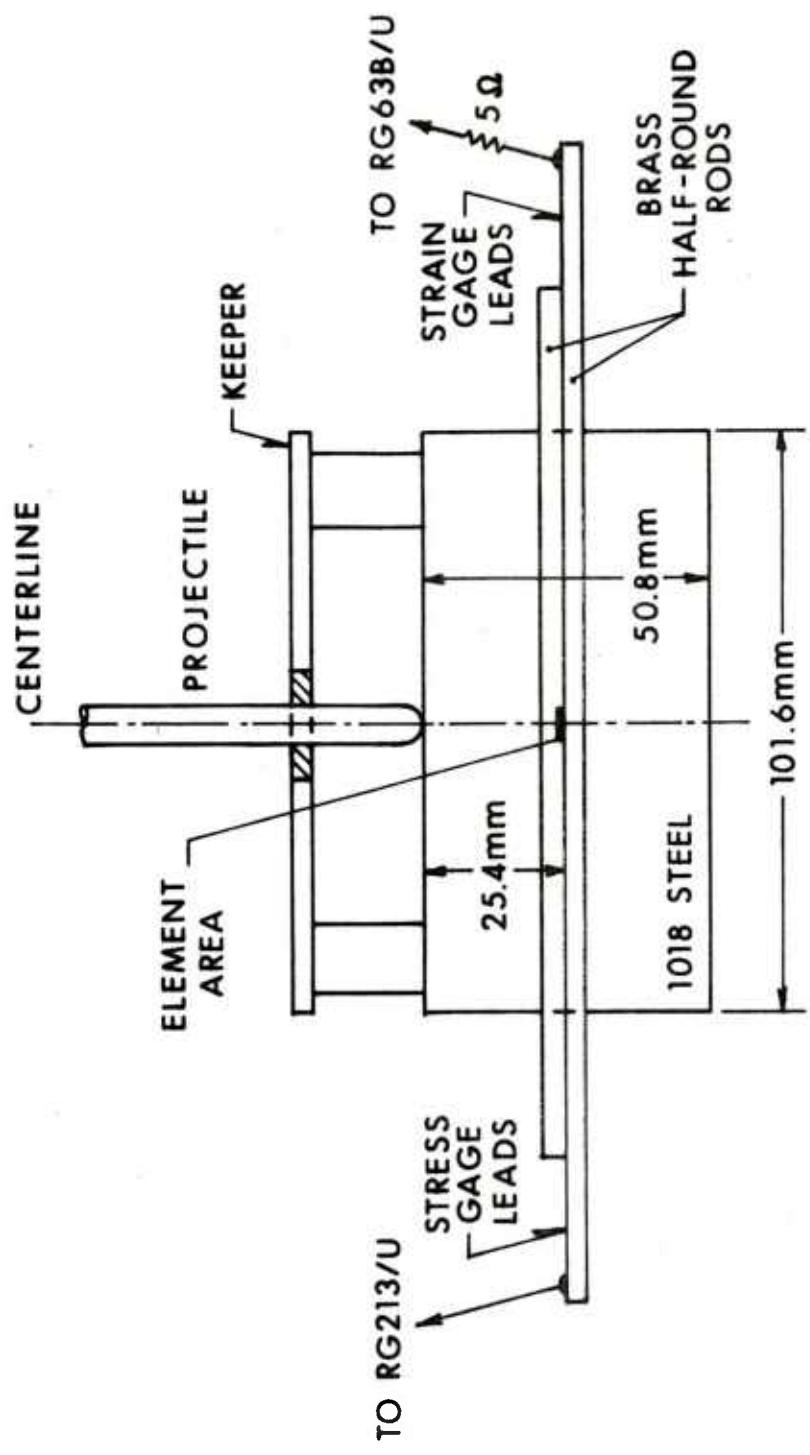


Figure 8. Tests 15 & 16 - Experimental Setups.

through the active element areas of the gauges. The second technique required the attachment of a mild steel keeper to the front of the target, as shown in Figure 8. This keeper allowed magnetic flux lines to "cycle" in the target portion ahead of the gauge element areas, further reducing the amount of noise-creating magnetic flux in these critical areas. This is the same principal that is applied when a keeper is placed on a permanent magnet to prevent the loss of its strength during storage. The keeper for a permanent magnet acts as a shorting path for magnetic flux lines. The keeper had a center hole which allowed the projectile to pass through it and strike the target. Quantitatively, it was not clear how much these shielding techniques aided in reducing the amount of noise in the monitored signals from the stress and strain gauge circuits. Qualitatively, these signals are the least noisy that have been obtained while using simple gauges in the type of magnetically disturbed environment which is encountered during penetration of steel targets.

The experimental results for Tests 15 and 16 were the best test results obtained so far in this test series. Stress-time and strain-time data from these tests are shown in Figure 9. The Test 15 results are represented by the stress and strain curves above the dotted lines. Because of a timing error made during the experiment, only the later parts of these test curves were recorded. Test 16 was an effort to duplicate Test 15 in its entirety. Because of a premature failure of the gauges for an unknown reason, only the two abbreviated curves below the dotted lines were obtained for Test 16. The dotted line portions connect the two experiments together extremely well. This connection strongly indicates that Test 15 was reproduced by Test 16. The strain-compensated stress curve was obtained as for Test 9. The strain-compensated stress achieves a steady state condition as time progresses, then begins to decrease rapidly as the penetrator nears the active element areas of the gauges. It is doubtful that this decrease to a final stress level of zero is real. As the measured stresses and strains recorded toward the end of the Test 15 record increase very rapidly, a large error factor is introduced in the calculation of the strain-compensated stresses. Also, the effect of the strain-compensated stress tending to zero toward the end of the experiment may only be an artifact of the onset of the destruction of the active gauge elements. The strain-compensated stress never rises above the Hugoniot Elastic Limit for mild steel (1.3 GPa)<sup>10,11</sup>.

---

<sup>10</sup>O. E. Jones, F. W. Neilson, and W. B. Benedick, "Dynamic Yield Behavior of Explosively Loaded Metals Determined by a Quartz Transducer Technique," J. Appl. Phys., Vol. 33, No. 11, November 1962, Fig. 3, p. 3228.

<sup>11</sup>O. E. Jones, and J. R. Holland, "Bauschinger Effect in Explosively Loaded Mild Steel," J. Appl. Phys., Vol. 35, No. 6, June 1964, pp. 1771-73.

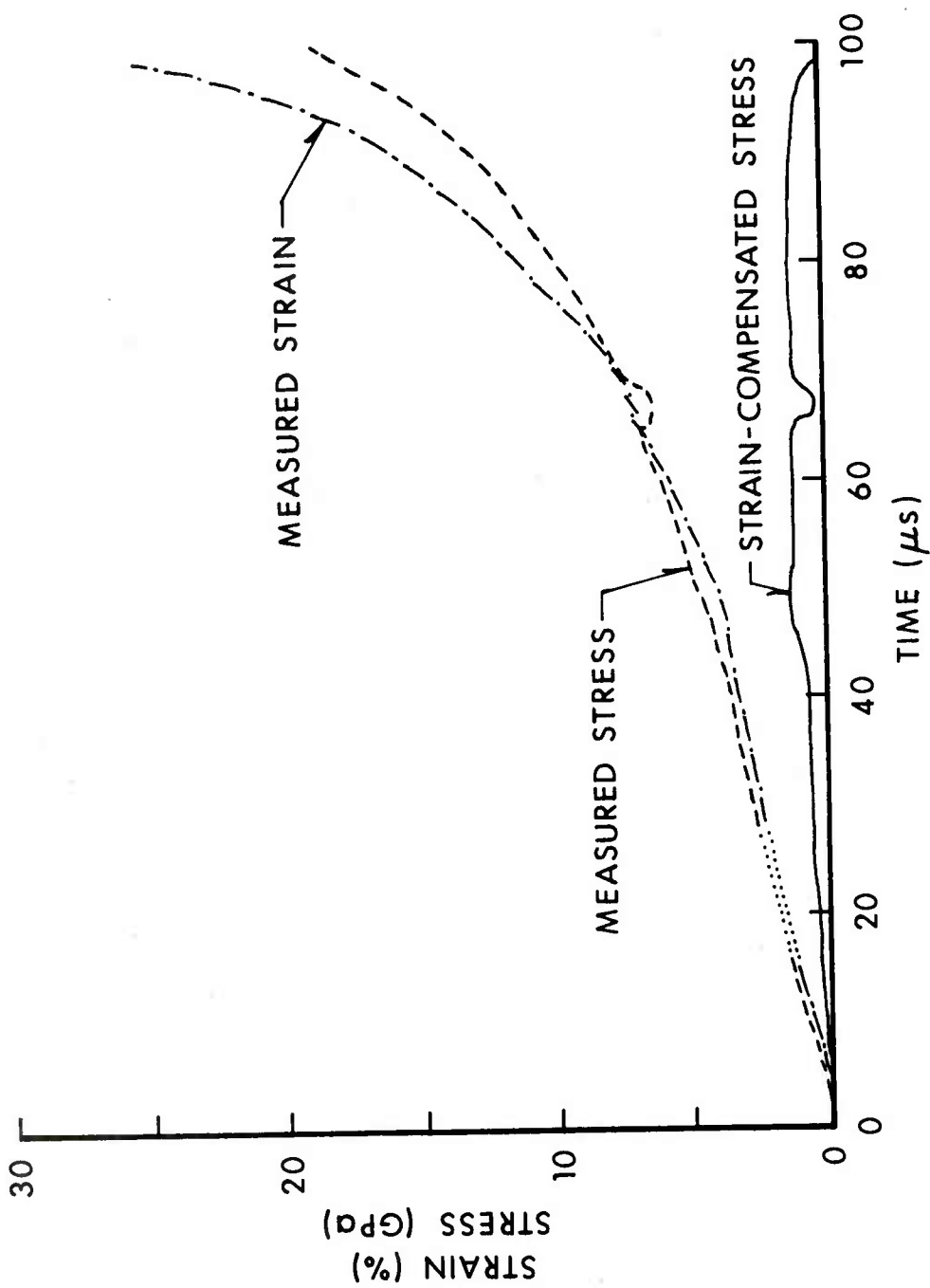


Figure 9. Stress and Strain Histories for Tests 15 & 16.

#### IV. SUMMARY AND CONCLUSION

Three very important results were obtained from the series of tests reported here. One was the fact that the use of the monobloc targets introduced for Test 13 and all subsequent tests produced better experimental results than the layered targets used in all experiments prior to Test 13. Two, during the evolution of these experiments, strain was found to affect gauges that were designed to respond to stress only. This effect was treated satisfactorily. Three, the achievement of obtaining reproducibility of results in identical tests was apparently attained for Tests 15 & 16, which enhances the reliability of these experiments.

More work remains to be done to characterize the phenomena occurring in these tests, and to relate them to other penetration phenomena on a theoretical and experimental basis. The point has been reached where meaningful and reproducible data are being obtained, so future plans are to continue experimentation with different target materials and arrangements. Several modifications and improvements are planned for these continuing experiments. Future plans include inserting more gauges into the monobloc targets at different depths. More data may thus be obtained from each test. Different thicknesses of RHA will be used again as target material. Some special gauges have been constructed which combine the stress and strain gauges as components of one complete gauge assembly\*. The gauge components have smaller active element areas than the separate gauges previously used. Also, the active elements of the component stress and strain gauges are constructed in an interlocking pattern rather than an overlapping one. This allows the active element areas of both the strain and stress components to be as integral as possible.

---

\*Developed by Dynasen, Inc.: Goleta, CA 93017.

#### **ACKNOWLEDGEMENTS**

G. E. Hauver and P. H. Netherwood are gratefully acknowledged for their many helpful suggestions and close support in connection with this series of tests.

## REFERENCES

1. H. Kolsky, *Stress Waves in Solids*, Dover Publications, Inc., New York, 1963, Plate I.
2. J. A. Charest, "Measurements of Hypervelocity Impact Pressures Using In-Material Manganin Gauges", EG&G Report S-487-R, Santa Barbara Division, April 1970.
3. J. A. Charest, "Development of a Strain-Compensated Shock Pressure Gauge", Dynasen, Inc. TR 005, February 1979.
4. A. V. Anan'in, A. N. Dremin, and G. I. Kanel', "Structure of Shock and Rarefaction Waves in Iron", *Fizika Gorgeniya i Vzryva*, Vol. 9, No. 3, May-June 1973, pp. 437-43.
5. E. O. Williams, "An Etched Manganin Gauge System for Shock-Pressure Measurement in a High-Noise Environment", *ISA Transaction*, Vol. 7, No. 3, 1968, pp. 223-30.
6. J. A. Charest, "Characterization of an Encapsulated 50-Ohm Manganin Foil Piezoresistive Gauge", Air Force Weapons Laboratory Technical Report No. AFWL-71-81, Kirtland Air Force Base, August 1972.
7. G. E. Hauer, "The Alpha-Phase Hugoniot of Rolled Homogeneous Armor", BRL Memorandum Report No. 2651, Ballistic Research Laboratory, Aberdeen Proving Ground, MD, August 1976, p. 14.
8. P. H. Netherwood, "Rate of Penetration Measurements", BRL Memorandum Report ARBRL-MR-02978, Ballistic Research Laboratory, Aberdeen Proving Ground, MD, December 1979, p. 15.
9. J. J. Trimble, "Manganin Gage Pressure Measurements Under Conditions Where Gage Deformation Occurs", BRL Technical Report ARBRL-TR-02180, Ballistic Research Laboratory, Aberdeen Proving Ground, MD, July 1979.
10. O. E. Jones, F. W. Neilson, and W. B. Benedick, "Dynamic Yield Behavior of Explosively Loaded Metals Determined by a Quartz Transducer Technique", *J. Appl. Phys.*, Vol. 33, No. 11, November 1962, Fig. 3, p. 3228.
11. O. E. Jones and J. R. Holland, "Bauschinger Effect in Explosively Loaded Mild Steel", *J. Appl. Phys.*, Vol. 35, No. 6, June 1964, pp. 1771-73.

DISTRIBUTION LIST

<u>No. of Copies</u>	<u>Organization</u>	<u>No. of Copies</u>	<u>Organization</u>
12	Commander Defense Technical Info Center ATTN: DDC-DDA Cameron Station Alexandria, VA 22314	1	Commander US Army Materiel Development and Readiness Command ATTN: DRCDLDD 5001 Eisenhower Avenue Alexandria, VA 22333
2	Director of Defense Research and Engineering Washington, DC 20301	3	Commander US Army Armament Research and Development Command ATTN: DRDAR-TSS (2 cys) DRDAR-SC, Dr. E. Bloore Dover, NJ 07801
2	Director Defense Advanced Research Projects Agency ATTN: Tech Info 1400 Wilson Boulevard Arlington, VA 22209	2	Commander US Army Armament Materiel Readiness Command ATTN: DRSAR-LEP-L, Tech Lib Rock Island, IL 61299
1	Director Weapon Sys Evaluation Group Washington, DC 20305	2	Director US Army Armament Research and Development Command Benet Weapons Laboratory ATTN: DRDAR-LCB-TL Dr. F. Schneider Watervliet, NY 12189
1	The National War College Fort Lesley J. McNair Fourth & P Streets, SW Washington, DC 20319	2	Commander US Army Aviation Research and Development Command ATTN: DRSAV-E P. O. Box 209 St. Louis, MO 63166
1	HQDA Deputy Assistant Secretary of the Army (R&D) Washington, DC 20310	1	Director US Army Air Mobility Research and Development Laboratory Ames Research Center Moffett Field, CA 94035
2	HQDA (DAMA-ARP; DAMA-MS) Washington, DC 20310		
1	Commander US Army Materiel Development and Readiness Command ATTN: DRCDMD-ST 5001 Eisenhower Avenue Alexandria, VA 22333		

DISTRIBUTION LIST

<u>No. of Copies</u>	<u>Organization</u>	<u>No. of Copies</u>	<u>Organization</u>
1	Director Applied Technology Laboratory US Army Research & Technology Laboratories (AVRADCOM) Fort Eustis, VA 23604	1	Commander US Army Natick Research and Development Command ATTN: DRXRE Natick, MA 01762
3	Commander US Army Communications Rsch and Development Command ATTN: DRDCO-PPA-SA DRSEL-HL-CT DRSEL-RD Fort Monmouth, NJ 07703	1	Commander US Army Tank Automotive Research & Development Cmd ATTN: DRDTA-UL Warren, MI 48090
1	Commander US Army Electronics Rsch and Development Command Technical Support Activity ATTN: DELSD-L Fort Monmouth, NJ 07703	7	Commander US Army Materials and Mechanics Research Center ATTN: DRXMR-ATL DRXMR-H, Mr. J. Dignam DRXMR-H, Dr. D. Dandekar DRXMR-H, Dr. S.C. Chou DRXMR-H, Dr. A.G. Martin DRXMR-T, Mr. J. Mescall DRXMR-T, Dr. R.P. Papirno Watertown, MA 02172
1	Commander US Army Harry Diamond Labs ATTN: DELHD-TA-L 2800 Powder Mill Road Adelphi, MD 20783	2	Commander US Army Research Office ATTN: Dr. Y. Horie Tech Lib P. O. Box 12211 Research Triangle Park NC 27709
1	Commander US Army Missile Command ATTN: DRSMI-R Redstone Arsenal, AL 35809	1	Commander US Army TRADOC Armor School Fort Knox, KY 40121
1	Commander US Army Missile Command ATTN: DRSMI-YDL Redstone Arsenal, AL 35809	1	Director US Army TRADOC Systems Analysis Activity ATTN: ATAA-SL, Tech Lib White Sands Missile Range NM 88002
2	Commander US Army Mobility Equipment Research & Development Cmd ATTN: DRDME-WC STSFB-MW Fort Belvoir, VA 22060		

DISTRIBUTION LIST

<u>No. of Copies</u>	<u>Organization</u>	<u>No. of Copies</u>	<u>Organization</u>
1	Commander US Army Command and General Staff College ATTN: ARCHIVES Fort Leavenworth, KS 66027	4	Commander Naval Weapons Center ATTN: Dr. M. E. Backman Dr. W. Goldsmith Dr. S. A. Finnegan Dr. K. G. Whitman China Lake, CA 93555
1	Commander US Army War College ATTN: Library Carlisle Barracks, PA 17013	2	Commander Naval Research Laboratory ATTN: Code 2020, Tech Lib Dr. W. J. Furguson 4555 Overlook Drive SW Washington, DC 20375
2	Commander US Military Academy ATTN: Library West Point, NY 10996	1	Superintendent Naval Postgraduate School ATTN: Director of Library Monterey, CA 93940
2	Office of Naval Research Department of the Navy ATTN: Code 402 Washington, DC 20360	3	AFWL (Tech Lib) Kirtland AFB, NM 87117
3	Commander Naval Air Systems Command ATTN: AIR-604 Washington, DC 20360	2	AFML (Dr. A. K. Hopkins; Tech Lib) Wright-Patterson AFB, OH 45433
3	Commander Naval Ordnance Systems Cmd Washington, DC 20360	4	Director Lawrence Livermore Laboratory ATTN: Dr. M. van Thiel, L-64 Dr. D. Banner, L-24 Dr. W. Von Holle Dr. W. H. Gust P. O. Box 808 Livermore, CA 94550
1	Commander & Director David W. Taylor Naval Ship Research & Development Ctr Bethesda, MD 20084	2	Los Alamos Scientific Lab ATTN: Dr. R. Karpp Tech Lib P. O. Box 808 Livermore, CA 94550
3	Commander Naval Surface Weapons Center ATTN: DX-21, Lib Mr. W. H. Holt Mr. W. Mock, Jr. Dahlgren, VA 22448		
2	Commander Naval Surface Weapons Center ATTN: Tech Lib Dr. J. W. Forbes Silver Springs, MD 20910		

DISTRIBUTION LIST

<u>No. of Copies</u>	<u>Organization</u>	<u>No. of Copies</u>	<u>Organization</u>
5	Los Alamos Scientific Lab ATTN: Dr. S. Goldstein Dr. C. E. Ragan Dr. L. R. Veeser Dr. J. W. Taylor Tech Lib P. O. Box 1663 Los Alamos, NM 87545	1	National Space Tech Labs ATTN: Tech Lib NSTL Station, MS 39529
7	Sandia Laboratories ATTN: Tech Lib Dr. W. Herrmann Dr. L. D. Bertholf Dr. P. Chen Dr. R. A. Graham Dr. C. W. Young Dr. J. W. Nunziato Albuquerque, NM 87115	1	Director National Science Foundation 1800 G Street, NW Washington, DC 20550
1	Headquarters National Aeronautics and Space Administration Washington, DC 20546	1	President National Academy of Science 2101 Constitution Avenue, NW Washington, DC 20418
2	Director NASA - Ames Research Center ATTN: Dr. J. L. Summers Technical Library Moffett Field, CA 94035	1	National Research Council 2101 Constitution Avenue Washington, DC 20418
1	Director Jet Propulsion Laboratory ATTN: Lib (TDS) 4800 Oak Grove Drive Pasadena, CA 91103	1	Library of Congress Technical Information Division Reference Department ATTN: Bibliography Section Washington 25, DC 20540
1	Director Lyndon B. Johnson Space Center ATTN: Lib Houston, TX 77058	1	Office of Technology Assessment US Congress ATTN: Mr. Coates Washington, DC 20510
2	Director NASA - Langley Research Center ATTN: Tech Lib Dr. E. H. Davison Langley Field, VA 23365	1	Aerojet General Corporation 11711 South Woodruff Avenue Downey, CA 90241
		2	Aerospace Corporation ATTN: Technical Library Dr. D. B. Singer P. O. Box 95085 Los Angeles, CA 90045
		2	Aircraft Armaments, Inc. Cockeysville, MD 21030

DISTRIBUTION LIST

<u>No. of Copies</u>	<u>Organization</u>	<u>No. of Copies</u>	<u>Organization</u>
1	AVCO Corporation Research and Advanced Development Division 201 Lowell Street Wilmington, MA 01887	1	Honeywell, Inc. Government & Aerospace Products Division ATTN: Dr. G. Johnson 600 Second Street, NE Hopkins, MN 55343
3	Battelle Columbus Labs ATTN: Dr. G. H. Brawley Dr. J. E. Backofen, Jr. Dr. J. H. Brown, Jr. 505 King Street Columbus, OH 43201	1	IIT Corporation ATTN: Mr. E. P. Bergmann 10 W. 35th Street Chicago, IL 60616
2	Boeing Aerospace Company ATTN: R. M. Schmidt J. E. Schrader P. O. Box 3999 Seattle, WA 98124	1	Kaman Sciences Corporation ATTN: Dr. D. C. Williams P. O. Box 7463 Colorado Springs, CO 80933
1	California Research & Tech, Inc. ATTN: Dr. D. L. Orphal 4049 First Street, Suite 135 Livermore, CA 94550	3	Ktech Corporation ATTN: Dr. V. Keller Dr. L. Lee Mr. D. A. Rice 911 Pennsylvania NE Albuquerque, NM 87110
1	Cannon Artillery Wpn Systems ATTN: Mr. M. F. Fisette 3708 Fernwood Court Davenport, IA 52807	2	Lockheed Palo Alto Research Laboratory 3251 Hanover Street Palo Alto, CA 94304
1	Dynasen, Inc. ATTN: Dr. J. A. Charest 20 Dean Arnold Place Goleta, CA 93017	1	McDonnell-Douglas Astronautics Company ATTN: Dr. J. Wall 5301 Bolsa Avenue Huntington Beach, CA 92647
1	Effects Technology, Inc. ATTN: Program Manager P. O. Box 30400 Santa Barbara, CA 93105	2	Physics International Company ATTN: Dr. E. T. Moore Mr. L. Behrmann 2700 Merced Street San Leandro, CA 94577
1	Falcon R&D Thor Facility 696 Fairmont Avenue Baltimore, MD 21204		

DISTRIBUTION LIST

<u>No. of Copies</u>	<u>Organization</u>	<u>No. of Copies</u>	<u>Organization</u>
3	Systems, Science, & Software ATTN: Dr. R. T. Sedgwick Ms. L. J. Hageman Dr. A. San Miguel P. O. Box 1620 La Jolla, CA 92037	3	Drexel Institute of Tech Wave Propagation Rsch Center ATTN: Prof. P. C. Chou 32nd and Chestnut Streets Philadelphia, PA 19104
1	Terra Tek, Inc. ATTN: Dr. Arfon Jones 420 Wahara Way University Research Park Salt Lake City, UT 84108	2	Illinois Inst of Tech 10 West 35th Street Chicago, IL 60616
1	TRW Systems One Space Park Redondo Beach, CA 90278	3	Johns Hopkins University Department of Materials Science and Civil Engineering ATTN: Prof. J. F. Bell Prof. R. Pond Dr. R. Green Maryland Hall Baltimore, MD 21218
1	Utah Research & Devel. Co. ATTN: W. N. Clark Salt Lake City, UT 84119	2	Applied Physics Laboratory Johns Hopkins University ATTN: Tech Lib Dr. G. H. Schlimm Johns Hopkins Road Laurel, MD 20810
1	Valpey Corporation P. O. Box 2311 Newport Beach, CA 92663	2	Massachusetts Inst of Tech 77 Massachusetts Avenue Cambridge, MA 02139
1	Whitaker Corporation Shock Hydrodynamics Division ATTN: Dr. Louis Zernow 4716 Vineland Avenue N. Hollywood, CA 91602	1	Michigan Technological Univ ATTN: Dr. W. W. Predebon Houghton, MI 49931
2	Brown University Division of Engineering Providence, RI 02192	1	Pennsylvania State Univ Engineering Mechanical Dept. University Park, PA 16802
2	California Institute of Tech Div of Engineering and Applied Science Pasadena, CA 91102	1	Rice University ATTN: Dr. C. C. Wang P. O. Box 1892 Houston, TX 77001
1	Denver Research Institute University of Denver ATTN: Dr. A. Krill Denver, CO 80210		

DISTRIBUTION LIST

<u>No. of Copies</u>	<u>Organization</u>	<u>No. of Copies</u>	<u>Organization</u>
3	Southwest Research Institute Dept of Mechanical Science ATTN: Dr. U. Lindholm Dr. W. Baker Mgr, Ballistic Tech 8500 Culebra Road San Antonio, TX 78228	6	University of Delaware Department of Mechanical and Aerospace Engineering ATTN: Dr. J. W. Edington Dr. Twu-Wei Chou Dr. J. E. Danberg Dr. R. B. Pipes Dr. J. R. Vinson Dr. Minoru Taya Newark, DE 19711
6	SRI International ATTN: Dr. G. R. Abrahamson Dr. D. Curran Dr. L. Seaman Dr. T. Rosenberg Dr. D. Erlich Dr. D. Shockey 333 Ravenswood Avenue Menlo Park, CA 94025	1	University of Utah High Velocity Laboratory Salt Lake City, UT 84111
2	Stanford University Center for Material Research Stanford, CA 94305	2	Washington State University Department of Physics ATTN: Prof. G. E. Duvall Pullman, WA 99163
1	University of California Department of Aerospace and Mechanical Eng. Science ATTN: Dr. Y. C. Fung P. O. Box 109 La Jolla, CA 92037	<u>Aberdeen Proving Ground</u> Dir, USAMSAA, Bldg. 392, APG-AA ATTN: DRXSY-D DRXSY-MP, H. Cohen Cdr, USATECOM, Bldg. 314, APG-AA ATTN: DRSTE-TO-F Dir, USACSL, Bldg. E3516, APG-EA ATTN: DRDAR-CLB-PA	

### USER EVALUATION OF REPORT

Please take a few minutes to answer the questions below; tear out this sheet, fold as indicated, staple or tape closed, and place in the mail. Your comments will provide us with information for improving future reports.

1. BRL Report Number \_\_\_\_\_

2. Does this report satisfy a need? (Comment on purpose, related project, or other area of interest for which report will be used.)  
\_\_\_\_\_  
\_\_\_\_\_  
\_\_\_\_\_

3. How, specifically, is the report being used? (Information source, design data or procedure, management procedure, source of ideas, etc.)  
\_\_\_\_\_  
\_\_\_\_\_  
\_\_\_\_\_

4. Has the information in this report led to any quantitative savings as far as man-hours/contract dollars saved, operating costs avoided, efficiencies achieved, etc.? If so, please elaborate.  
\_\_\_\_\_  
\_\_\_\_\_  
\_\_\_\_\_

5. General Comments (Indicate what you think should be changed to make this report and future reports of this type more responsive to your needs, more usable, improve readability, etc.)  
\_\_\_\_\_  
\_\_\_\_\_  
\_\_\_\_\_

6. If you would like to be contacted by the personnel who prepared this report to raise specific questions or discuss the topic, please fill in the following information.

Name: \_\_\_\_\_

Telephone Number: \_\_\_\_\_

Organization Address:  
\_\_\_\_\_  
\_\_\_\_\_